Available online at BCREC website: https://bcrec.id

Bulletin of Chemical Reaction Engineering & Catalysis, 17 (2) 2022, 383-393

Research Article

Synthesis Metal-Organic Framework (MOFs) Cr-PTC-HIna Modulated Isonicotinic Acid for Methylene Blue Photocatalytic Degradation

Adawiah Adawiah[1], Wulandari Oktavia[2], Nanda Saridewi[3], Farhan Maulana Azhar[2], Risma Nur Fitria[2], Muhammad Shofyan Gunawan[2], Sri Komala[2], Agustino Zulys[4,*]

[1]Integrated Laboratory Centre, Faculty of Science and Technology UIN Syarif Hidayatullah Jakarta, Jl. Ir. H. Juanda No. 95 Ciputat Tangerang Selatan 15412, Indonesia.
[2]Department of Chemistry, Faculty of Science and Technology UIN Syarif Hidayatullah Jakarta, Jl. Ir. H. Juanda No. 95 Ciputat Tangerang Selatan 15412, Indonesia.
[3]Department of Chemistry Education, Faculty of Tarbiya and Teaching Sciences, UIN Syarif Hidayatullah Jakarta, Jl. Ir. H. Juanda No. 95 Ciputat Tangerang Selatan 15412, Indonesia.
[4]Department of Chemistry, Faculty of Mathematics and Natural Sciences, University of Indonesia, Jl. Lingkar Kampus Raya, Pondok Cina, Beji, Depok, Jawa Barat 16424, Indonesia.

Received: 24th March 2022; Revised: 29th April 2022; Accepted: 30th April 2022
Available online: 6th May 2022; Published regularly: June 2022

Abstract

A novel responsive visible light Cr-based MOF, Cr-PTC-HIna, was synthesized using the solvothermal method. Cr-PTC-HIna peaks were observed at 2θ = 9.04°, 12.71°, 14.88°, 25,48°, 27.72°, 28.97°, and 43.60° with a crystal size of 21 nm. Band gap energy achieved from the Cr-PTC HIna was 2.05 eV. Scanning Electron Microscope (SEM) analysis obtained a 3D structural morphology of MOFs Cr-PTC-HIna with a cylindrical tube shape and a particle size of 251.45 nm. Cr-PTC-HIna gave the optimum methylene blue degradation at pH of 7 under 250 watts mercury lamp irradiation for 180 minutes with degradation capacity of 95.40 mg/g. Electron holes and hydroxyl radicals were found as the dominant species contributing to methylene blue degradation.

Keywords: Isonicotinic acid; methylene blue; Cr-PTC-HIna; photocatalyst; solvothermal

How to Cite: A. Adawiah, W. Oktavia, N. Saridewi, F.M. Azhar, R.N. Fitria, M.S. Gunawan, S. Komala, A. Zulys (2022). Synthesis Metal-Organic Framework (MOFs) Cr-PTC-HIna Modulated Isonicotinic Acid for Methylene Blue Photocatalytic Degradation. *Bulletin of Chemical Reaction Engineering & Catalysis*, 17(2), 383-393 (doi:10.9767/bcrec.17.2.13930.383-393)

Permalink/DOI: https://doi.org/10.9767/bcrec.17.2.13930.383-393

1. Introduction

Dye wastewater level has been increasing in the environment since the dyes have been used extensively in the industries. The contaminant plays a prominent role in environmental pollution if disposed of without prior treatment due to its difficulty in naturally decomposed [1]. Several methods have been expanded for dye contaminant degradation, including coagulation, adsorption, flocculation, and photocatalytic [2]. Photocatalytic is the most widely developed method for dye degradation because it is considered the most effective, low cost, and environmentally friendly. The end products of the photocatalytic method are CO_2 and H_2O [3]. In general, materials that are advantageous as photo-

* Corresponding Author.
Email: zulys@ui.ac.id (A. Zulys)

catalyst materials are semiconductor and some organic compounds [4].

Metal-Organic Frameworks (MOFs) are new porous crystalline materials constructed of metal ions and organic linkers connected through coordination bonds. The advantage of MOFs in dye photocatalytic degradation is due to large surface area, abundant pores and active sites, and high stability in aqueous, acidic, and basic systems [5]. However, MOFs have a limitation, such as the fast recombination rate that generates the reduction of catalytic activity of MOFs. The recombination rate happens when the excited electrons in the conduction band return to the electron holes in the valence band. Adding modulator compounds into MOFs is one of the strategies to inhibit this process. The addition of modulator into MOFs forms micropores particles, thereby indirectly inhibiting the recombination rate of MOFs [6]. Cai and Jiang reported an enlarged MOF Zr-BCD pore due to the incorporation of a monocarboxylic acid modulator to increase its catalytic activity in dyes degradation [7]. Another research also reported also reported that MIL-53 with HCl modulator provided escalated surface area specifications that showed more adsorptive and catalytic sites. Its photocatalytic activity was enhanced 1.5 times to MIL-53 without a modulator [8].

Isonicotinic acid is a pyridine carboxylate compound, where the carboxylic group resides at position 4 [9]. The presence of carboxylic groups and nitrogen in the structure of isonicotinic acid causes it to be an excellent linker to build various coordination complexes [10]. The addition of isonicotinic acid increase MOFs' size and pores volume, which enhances their catalytic activity [11]. Zhou *et al.* reported nanoporous MOFs $[Co_4(CH_3COO)(in)_5(\mu 3\text{-}OH)_2].2H_2O$ for CO_2 adsorption [12].

Perylene-3,4,9,10-tetracarboxylic is an organic linker that was used to develop MOFs material. Perylene-3,4,9,10-tetracarboxylic can reduce MOFs' band gap energy due to the aromatic ring's conjugated bond on it so that it is responsive to visible light. High-stability MOFs are constructed by selecting metal ions and organic linkers based on Pearson's hard/soft acid/base (HSAB) principles. The HSAB principle explains that ligands based on carboxylate groups are hard-bases and interact strongly with metal ions with hard-acidic properties like Cr^{3+} [13].

Therefore, this study aims to synthesize metal-organic frameworks (MOFs) which the building blocks consist of Cr^{3+} metal ion, perylene-3,4,9,10-tetracarboxylic ion, and isonicotinic acid for methylene blue degradation under visible light irradiation.

2. Materials and Methods

2.1 Preparation of Na_4PTC from PTCDA

The conversion process was carried out by mixing PTCDA (0.5 g 1.27 mmol) and NaOH (0.356 g, 8.9 mmol) in 50 mL of distilled water. The mixture was made to be homogenic by magnetically stirring at 300 rpm for one hour. The greenish solution was filtered and added excess ethanol to form yellow precipitate. The product was washed with excess ethanol to a neutral pH, and dried at room temperature overnight.

2.2 Synthesis of Cr-PTC MOF Modulated by Isonicotinic Acid (Cr-PTC-HIna)

Cr-PTC-HIna were synthesized by mixing $CrCl_3.3H_2O$ (2 mmol), Na_4PTC (1 mmol), and isonicotinic acid (0.5 mmol) in 25 mL distilled water and 5 mL DMF. Then, the mixture was magnetically stirred at 300 rpm for one hour, then placed to Teflon-lined stainless steel autoclave and heated at 170 °C for 24 hours. The precipitate formed was filtered and washed with distilled water, then dried for 24 hours at 70 °C. The final products were designated as Cr-PTC-HIna.

2.3 Characterization of Cr-PTC-HIna

The crystallinity and crystal size of sample was investigated by X-Ray diffraction spectroscopy (7000 Maxima-X). The functional groups were analyzed by FTIR (Prestige 21 Shimadzu), band gap energy was measured by UV-Vis DRS UV-Vis Spectrophotometer Agilent Carry 60 with $BaSO_4$ as a reference at the wavelength of 200-800 nm. The morphology of sample was obtained by SEM analysis on an FEI Quanta 650.

2.4 Methylene Blue Degradation Analysis

25 mg of Cr-PTC-HIna were dispersed into 50 mL of methylene blue solution and then magnetically stirred at 300 rpm at room temperature for 3 hours in the dark and under 250 watts of mercury lamp irradiation as a visible light source. Furthermore, the suspension was sampled as much as 2.0 mL every 30 minutes, then centrifuged at 6000 rpm for 10 minutes. The concentration of methylene blue was measured using a UV-Vis spectrophotometer at 665 nm. The efficiency of methylene blue degradation is calculated using the following equation:

$$DC\ (mg/gram) = \frac{C_0 \times (A_0 - A_t) \times V}{m \times 100} \quad (1)$$

where, DC (mg/gram) is degradation capacity of Cr-PTC-HIna (mg MB/gram Cr-PTC-HIna), C_0 is initial MB concentration, A_0 is absorbance of initial MB concentration, A_t is absorbance of final MB concentration, V is volume of MB solution (L), m is dosage of Cr-PTC-Hina (gram).

The optimum photocatalytic activity was measured by using several parameters, including the initial methylene blue concentration of 25, 50, and 75 ppm, Cr-PTC-HIna dosage of 15, 25, 35, and 45 mg, and pH of 2, 5, 7, 9, and 11. A fixed amount of H_2O_2, CH_3OH, and tert-butanol was added to determine the dominant species in the photocatalytic degradation of methylene blue.

3. Results and Discussion

3.1 X-Ray Diffraction of Cr-PTC-HIna

The crystallinity of Cr-PTC-HIna is essential to know, considering its application as photocatalyst. The photocatalyst crystallinity dramatically affects the photocatalytic reaction rate. Figure 1 explained that Cr-PTC-HIna have good crystallinity with the main diffraction peaks at 2θ = 9.04°, 12.71°, 25.48°, and 27.72°. The indexes of Cr in Cr-PTC or Cr-PTC-HIna cannot be presented since we assumed that it is the novel material, and the single crystal was not obtained. We assumed that it is the new material based on the diffraction peak intensities between Cr-PTC and Cr-PTC-HIna.

The XRD patterns show almost no difference among pure Cr-PTC with modulated MOF Cr-PTC-HIna. It confirmed the crystalline structure of Cr-PTC was preserved after being modulated by isonicotinic acid. The effect of isonicotinic acid on the MOFs structure was to change several ligands or linkers from the MOFs without changing the entire structure of the MOFs. This can be proved by the insignificant transformation of the intensity from the diffraction patterns. If the structure is entirely changed, then the isonicotinic acid will form peaks with significant intensity and the diffraction pattern of Cr-PTC *vs* Cr-PTC-HIna was completely different.

Cr-PTC-HIna crystallinity was affected by solvothermal with a mixture of water and DMF as the solvent that was employed to synthesize it. DMF serves the MOFs' crystal growth by converting DMF into suitable amines at high-temperature. It controlled the deprotonation level of carboxylate linkers [14] and the solvothermal method used a temperature above the solvent's boiling point to control the rate of crystal growth by reducing the activation energy barrier in the reaction of metal ions with organic linkers [15].

XRD characterization also provides crystal size that was measured using the Debye Scherer equation:

$$D = \frac{k\lambda}{\beta \cos\theta} \quad (2)$$

Measuring crystal size was calculated by taking peaks with a high-intensity value, namely the peak at 2θ = 12.71° [2] of 1780 cps. From the Debye Scherer equation, the crystal size of the Cr-PTC-HIna is 21 nm and smaller than Cr-PTC without an isonicotinic acid is 25.7 nm.

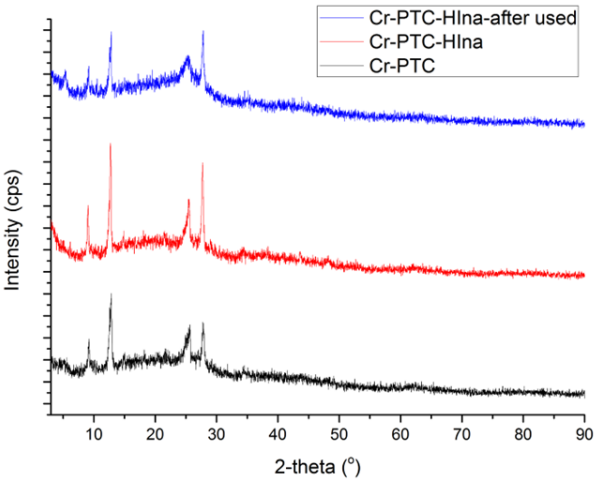

Figure 1. Diffractogram pattern of Cr-PTC and Cr-PTC-HIna (before and after used)

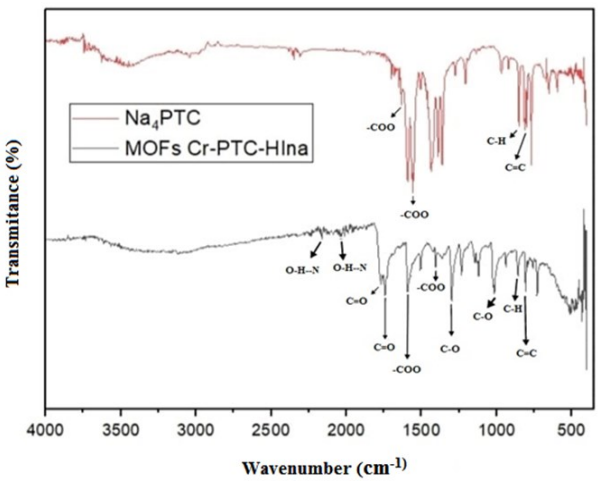

Figure 2. FTIR spectra of Na_4PTC and Cr-PTC-HIna.

3.2 FTIR Spectrum and Functional Group of MOFs Cr-PTC-HIna

The FTIR spectrum of MOFs Cr-PTC-HIna shows that the absorption peaks are at wavenumbers 4000–400 cm^{-1} (Figure 2). The bands are observed at 1769 cm^{-1} and 1742 cm^{-1} corresponding to asymmetric and symmetric stretching vibrations (C=O). The bands at 1299 cm^{-1} and 938 cm^{-1} were attributed to asymmetric and symmetric stretching (C–O) vibrations. In addition, broad absorption bands at 2039 and 2161 cm^{-1} assigned the existence of an intermolecular hydrogen bond (OH---N) between H_2O in the system and the nitrogen group of isonicotinic acid [17], which suggested that the N pyridil atom is not coordinated to the central chromium ion. However, the absence of an absorption band of –COOH group also indicates that the –COO group in isonicotinic acid has been coordinated with Cr^{3+} to form Cr–COO. Those peaks were not found in Na_4PTC. Then, the bands at 1423 cm^{-1} and 1633 cm^{-1} of Na_4PTC shifted to 1406 cm^{-1} and 1591 cm^{-1} at Cr-PTC-HIna corresponding to symmetric (O–C–O) vibration, thus confirming the presence of PTC (perylene-3,4,9,10-tetracarboxylate) linker within the Cr-PTC-HIna framework structure. The observed peak at 545 cm^{-1} is correlated with Cr–O vibration. Roosta *et al.* explained that stretching vibration of oxygen with metal is generally detected in the range of 400–800 cm^{-1} [16]. The other bands between 1600–600 cm^{-1} are attributed to aromatic rings, including the stretching vibration (C=C) at 1506 cm^{-1} and deformation stretching vibration (C–H) in plane at 1234, 1143, 1119, and 1015 cm^{-1}. The bands at 857 and 807 cm^{-1} corresponded to bending vibration (C–H) out of plane 1,2,3,4-tetrasubstituted aromatic ring. The bending vibration (C=C) out of plane aromatic ring at 757 cm^{-1} and 730 cm^{-1}.

3.3 Band Gap Energy (E_g) of Cr-PTC-HIna

Bandgap energy is the energy between the valence band and conduction band that represents the maximum energy in the electrons' excitation process. Based on the calculations using Kubelka Munk and Tauc plots, the bandgap energy of Cr-PTC-HIna is 2.05 eV (Figure 3). It absorbs maximum light up to a wavelength of 604 nm, therefore Cr-PTC-HIna is a responsive visible light semiconductor material.

The low bandgap energy of MOFs Cr-PTC-HIna was influenced by π–π* electronic transition on the conjugated bond of the perylene linker ligand used. Jiang *et al.* synthesized MOFs Ni-BDC with bandgap energy of 3.12 eV [18]. Zulys *et al.* reported Ni-MOFs (Ni-PTC) gave smaller bandgap energy of 2.41 eV [19]. Bandgap energy of Ni-MOFs is smaller than that of benzenedicarboxylate due to perylene having more aromatic rings (five rings) than benzene (one ring). The more aromatic rings in the ligand lead degree of conjugation were high. As a result, increasing conjugation shifts the spectrum toward longer wavelength absorptions.

Besides that, the size of the secondary building unit (SBU) of the metal ion also affected the bandgap energy of MOFs [20]. The larger the SBU size of MOFs, the narrower bandgap energy. The size of SBU increased as the number of electrons increased. The increasing number of electrons affects the number of electrons at the HOMO energy level and delivers to the narrower energy level between valence and conduction band. The MOFs Y-PTC

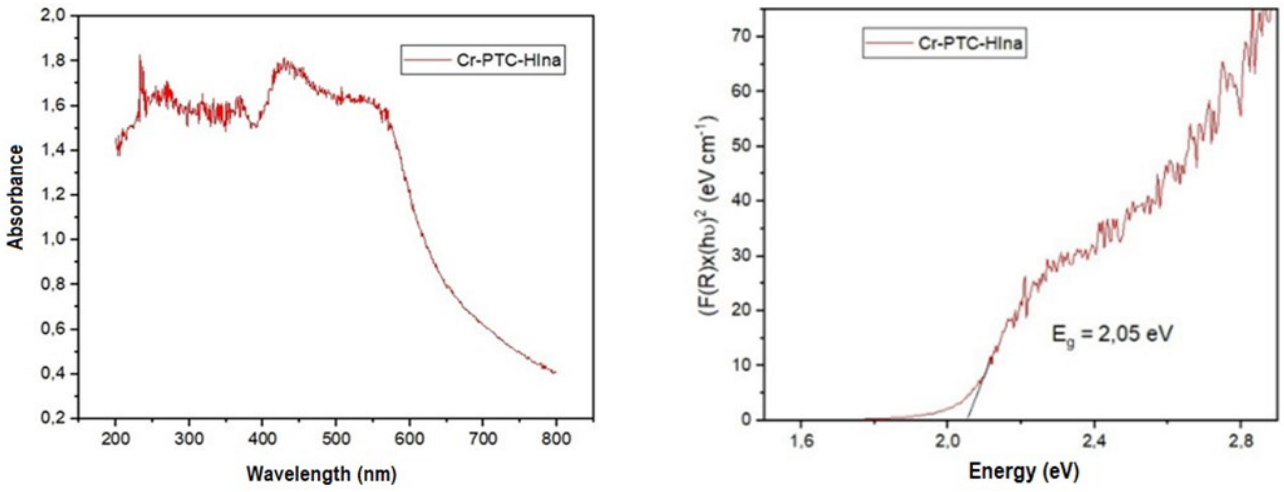

Figure 3. DRS-UV spectra and Tauc plot of Cr-PTC-HIna-2.

was synthesized by solvothermal method with a bandgap energy of 2.20 eV [21, whereas band gap energy of Cr-PTC is smaller than the band gap energy of Y-PTC that is 2.01 eV (previous study).

The other factor that can affect the energy of the bandgap is particle size. Adding isonicotinic acid modulator in the Cr-PTC reduces MOFs particle size. The decreased particle size causes the charge carriers of MOFs to interact quantum mechanically. It leads to a discrete electrolytic state which increases bandgap energy and a shift in band edge [22]. Lin *et al.* explained that the factors that affect bandgap are derived from ligands, SBU size, and particle size and come from electronic effects, crystal defects, and impurities [20].

3.4 The Morphology of Cr-PTC-HIna

Figure 4 illustrates Cr-PTC-HIna that was 3D metal-organic frameworks with a cylindrical tube shape. The particle size of Cr-PTC-HIna can be determined by looking at SEM data calculated by imageJ™ and Origin Pro™ softwares. The particle size of Cr-PTC-HIna was 251.45 nm smaller than MOFs Cr-PTC, which was 337 nm (previous study). Cr-PTC-HIna belongs to nanoparticle material with a size range of 10-1000 nm [23]. The carboxylate group in the Na_4PTC competes with isonicotinic acid in the MOFs network formation. The competition of carboxylate groups impacts crystal growth where large particle sizes are difficult to achieve, enhancing the formation of MOFs with smaller particle sizes [24].

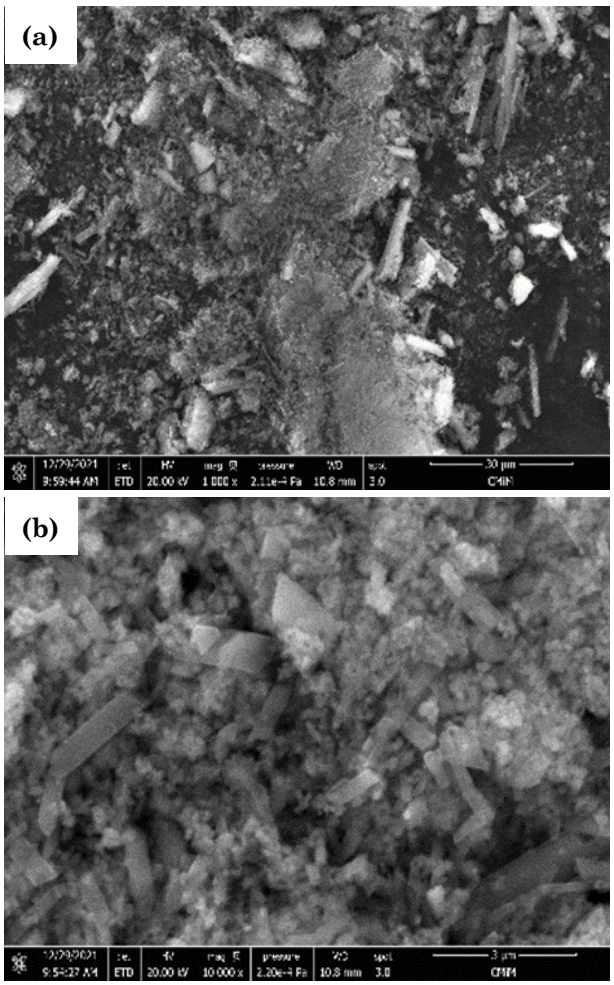

Figure 4. Morphology of Cr-PTC-HIna with (a) 1000x, and (b) 10000x magnification.

3.5 Methylene Blue Degradation by Cr-PTC-HIna

Figure 5 shows that Cr-PTC-HIna degraded methylene blue higher than Cr-PTC either in light or dark conditions. Both Cr-PTC and Cr-PTC-HIna degrade methylene blue in two mechanisms, namely adsorption, and photocatalytic mechanisms. The adsorption of methylene blue by MOFs occurs through several interactions, including electrostatic, hydrophobic, acid-base, π–π, and hydrogen bonds interaction or a combination of these interactions [25]. Mantasha *et al.* demonstrate that Cu-BTC-1 (Cu metal ion-based MOFs and benzene tricarboxylate linkers) could adsorb methylene blue using electrostatic interactions, π–π interactions, and hydrogen bonding [26]. Similar to Cu-BTC-1, adsorption between MB and Cr-PTC-HIna ensues via a combination mechanism between electrostatic interactions, hydrogen bonds, and π–π interactions.

The electrostatic interaction of Cr-PTC-HIna on methylene blue takes place between the positive charge of methylene blue located on the nitrogen atom (N) and sulfur atom (S) with the negative charge on π bonding in the

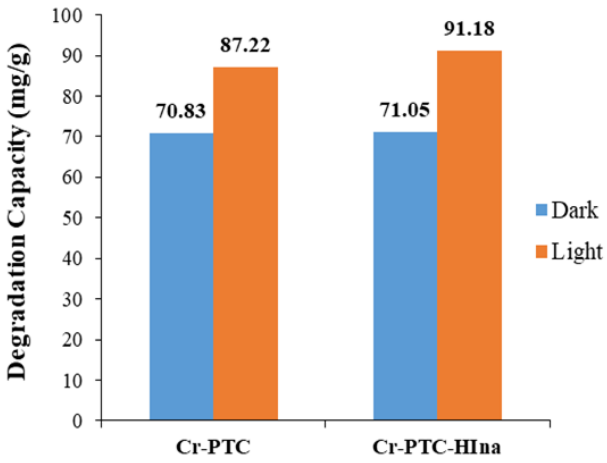

Figure 5. Degradation capacity of methylene blue by Cr-PTC and Cr-PTC-HIna.

benzene ring of Cr-PTC-HIna (charge-balancing anion). Furthermore, π–π interaction between Cr-PTC-HIna and methylene blue comes to pass between the π bonding in the aromatic ring of methylene blue and the aromatic ring of perylene in Cr-PTC-HIna. Meanwhile, the hydrogen bonding interactions come about between hydrogen in methylene blue and oxygen in carboxylic groups in Cr-PTC-HIna, or hydrogen in methylene blue and nitrogen pyridine ring in isonicotinic acid in Cr-PTC-HIna (Figure 6).

Figure 5 revealed Cr-PTC-HIna has photocatalytic activity in methylene blue degradation with degradation capacity 91.18 mg MB/g MOFs under visible light irradiation for 180 minutes. The isonicotinic acid is involved in a linker competitor toward perylene, replacing some existing perylene in the Cr-PTC. The perylene replacement by an isonicotinic acid modulator, then formed smaller particle sizes MOFs [27]. MOFs with smaller particle sizes increase the surface area of MOFs. It brings about escalating the pores containing active sites that contributed to enhancing photocatalytic activity [28].

Adding isonicotinic modulator in MOFs affected MOFs crystallinity and crystal size (see the XRD analysis). It generates the photocatalytic reaction, especially in the separation and electron migration steps. High crystallinity impacts the fewer crystal defects formed. Crystal defects are excited electron and electron hole trapping agents that will decrease photocatalytic activity. Hence, lowering crystal defects reduces the recombination rate and increase the photocatalytic activity [29]. On the other hand, the reduction of MOFs' crystal size affected the distance of excited electrons and electron holes migrating to the reaction site on the photocatalyst surface to be shorter, which inhibits the recombination rate between excited electrons and electron holes due to the faster migration of charge carriers and electron holes.

3.6 The Effect of Methylene Blue Initial Concentration

Figure 7 illustrate the degradation capacity of Cr-PTC-HIna for 180 min under visible light

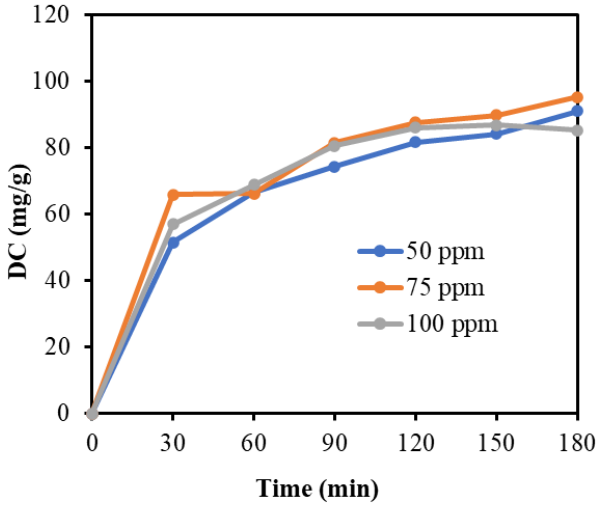

Figure 7. Degradation capacity Cr-PTC-HIna in various methylene blue initial concentration.

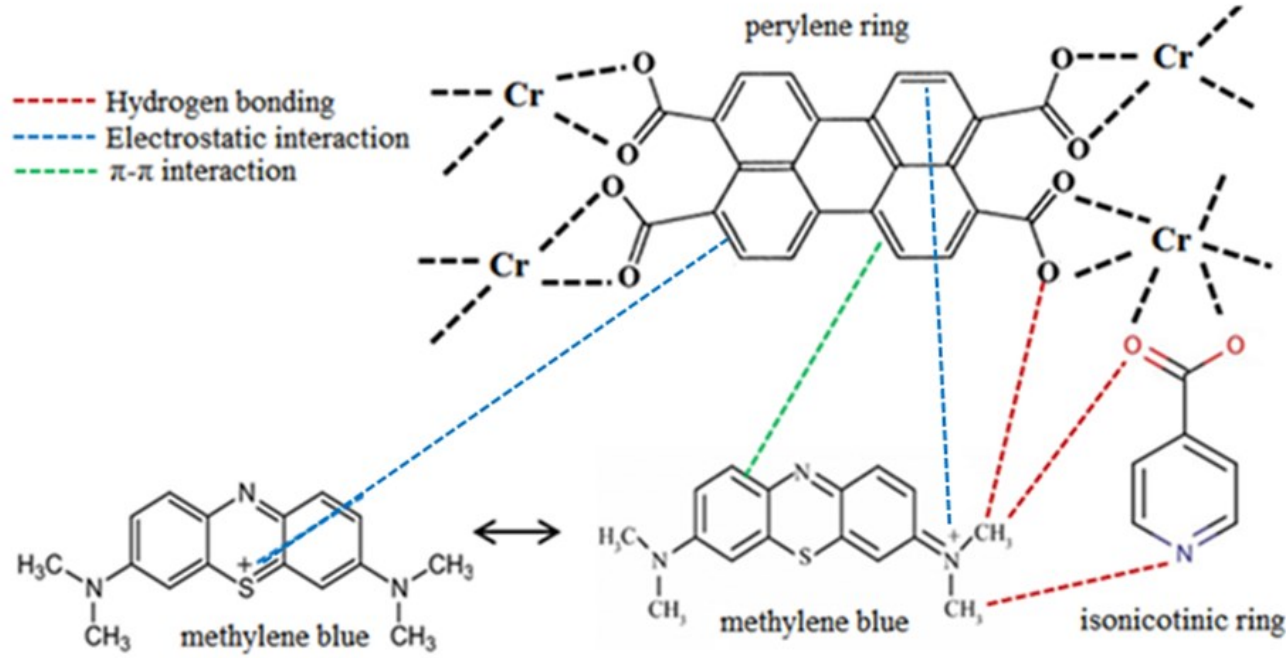

Figure 6. Possible interactions between methylene blue and Cr-PTC-HIna.

irradiation at MB initial concentration of 50 ppm was 91.18 mg/g, followed by 75 ppm at 95.40 mg/g and 100 ppm at 85.46 mg/g. Hence, the methylene blue initial concentration of 75 ppm is the optimum concentration. Figure 7 exhibits Cr-PTC-HIna in MB initial concentration of 100 ppm has no photocatalytic activity. Thus, the degradation of MB was occurred by the adsorption-desorption mechanism. It can be seen from the degradation graph, which does not change MB degradation significantly and tends to decrease after 150 minutes of reaction time. Decreasing degradation capacity at 100 ppm could be caused by the increase of methylene blue molecules attached to the surface of Cr-PTC-HIna, thus making the surface closed. It generated photon energy not to penetrate Cr-PTC-HIna layer, and the electron excitation process keep off [30]. On the other hand, methylene blue can absorb light, as a result increasing methylene concentration reduces the intensity of light entering the system. Therefore, photocatalytic reactions are challenging to achieve.

The effect of concentration was also shown by Samuel *et al.* [30]. He and his co-worker reported the addition of 4-nitrophenol concentration from 5 mg/L to 10 mg/L resulted in increased degradation capacity of MOFs [Zn(BDC)(DMF)]. However, when the concentration was increased to 40 mg/L, the degradation efficiency was decreased significantly. Another researcher also demonstrated that increasing the concentration of dye from 20 mg/L to 60 mg/L increased the degradation capacity. However, the concentration was increased to 100 mg/L, and the degradation capacity was decreased [31].

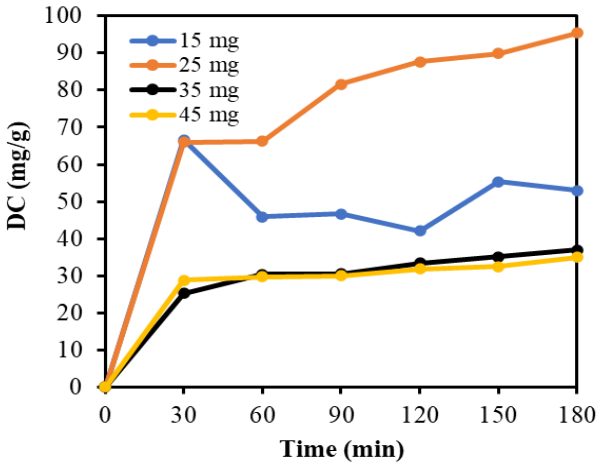

Figure 8. Degradation capacity of Cr-PTC-HIna in variation of MOFs Cr-PTC-HIna dosage.

3.7 The Effect of Cr-PTC-HIna Dosage

Figure 8 represents the degradation capacity of Cr-PTC-HIna was affected by the dosage of dispersed photocatalyst, which increasing Cr-PTC-HIna dosage from 15 mg to 25 mg improving MB degradation. The enhancement of Cr-PTC-HIna's dosage contributed to the number of active sites to degrade methylene blue. Nevertheless, the rising Cr-PTC-HIna dosage from 25 mg to 45 mg showed a declining MB degradation. Replenishment of Cr-PTC-HIna dosage exceeded the maximum photocatalyst dosage limit caused the solution to form a colloidal system. It impacts the occurrence of a fall off the penetration of light in the system [32]. The same effect is also reported by Samuel et al. [30] who was in his study using a variations of MOFs [Zn(BDC)(DMF)] dosage of 0.25–1.0 g/L gave the optimum degradation at 0.5 g/L.

3.8 The Effect of pH

Figure 9 proves that lowering pH will decrease MB degradation activity. It was involved by increasing H^+ ion affected to the protonation of Cr-PTC-HIna which becomes less negatively charged. The protonation of Cr-PTC-HIna arise at the nitrogen atom in isonicotinic acid and the carbon atom in the aromatic ring of the perylene. Acids with a pH of 2 show lower degradation activity than acids with a pH of 5 because excess H^+ ions in the system will protonate Cr-PTC-HIna to become more positively charged, bringing on repulsion interaction between Cr-PTC-HIna and cationic dye methylene blue. It leads to lower adsorption efficiency of methylene blue by MOFs [26].

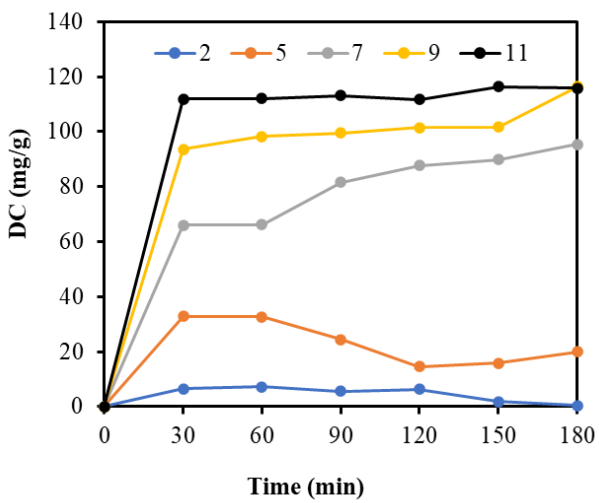

Figure 9. Degradation capacity of Cr-PTC-HIna in the variation of pH.

The MB degradation process was started from the adsorption of methylene blue to the active site contained in pores of MOFs. The adsorbed MB molecules are photodegraded in the MOFs active site, and finally, the degradation products are desorbed into the system. Reducing the adsorbed methylene blue molecules on MOFs reduces photocatalytic activity indirectly.

It is different in alkaline conditions, the MB degradation increased from neutral to pH of 11 (Figure 9). However, the escalation of MB degradation at alkaline pH is non-optimal pH. At pH 9 and 11, the percent degradation of methylene blue climbed insignificantly from the first 30 to 180 minutes of reaction time. The dominant activity at alkaline pH conditions of 9 and 11 is adsorption activity. It is supported by the analysis result in the dark condition in both alkaline pH of 74.06% and 76.19%, which are not much different from the light conditions of 77.56% and 77.24%. The enhancement of alkaline pH-induced deprotonates of MOFS leads to becoming more negatively charged. The more negatively charged MOFs will strongly interact with the methylene blue cationic dye and produce higher adsorption activity [26].

In addition, the alkaline pH decompose Cr-PTC-HIna which was indicated by a change in the color of the solution from blue to green (Figure 10). The addition of alkaline solution (NaOH) induced decomposition of Cr-PTC-HIna to produce chromium(III) hydroxide $(Cr_3OH)_6^{3+}$ complex (Equation 3).

$$Cr\text{–}PTC\text{-}HIna_{(s)} + OH^-_{(aq)} \rightarrow Cr(OH)_6^{3+}{}_{(aq)} + PTC^- + Hina \quad (3)$$

At pH of 7, MOFs Cr-PTC-HIna showed the highest photocatalytic activity to methylene blue degradation. It is due to Cr-PTC-HIna have good adsorption capacity of methylene blue and stability in pH of 7. The principle of hard, soft acid-base (HSAB) explains that MOFs were constructed from hard acid (carboxylate group), and hard base (high valence metal ion like Cr^{3+}) provide good stability in neutral and acidic pH conditions [13]. The stability of Cr-PTC-HIna can be seen from the XRD pattern of MOFs after being used (Figure 1).

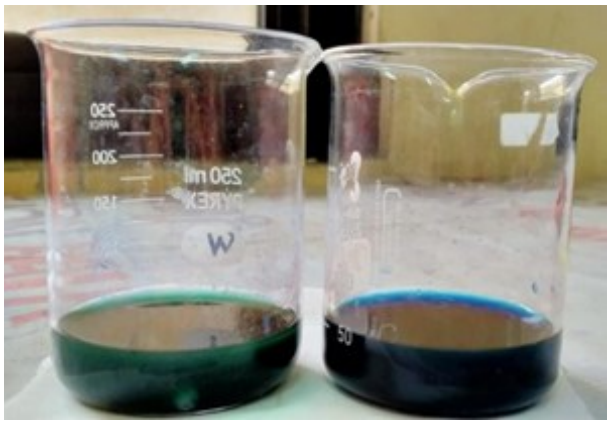

Figure 10. Methylene blue solution dispersed by Cr-PTC-HIna under alkaline conditions (pH 11) (left) and acidic solution (pH 2) (right).

3.9 The Effect of Electron-Hole Scavenger

Generally, the photocatalytic methylene blue degradation mechanism can be illustrated in Figure 11. When photon energy is irradiated on Cr-PTC-HIna surface (i), the electrons from the filled valence band are excited to the conduction band, forming electron-hole pair (ii). Then, photogenerated holes oxidize water molecules or hydroxide ions from dissociated H_2O_2 into reactive radical •OH for MB degradation (iiia). Meanwhile, the electron-hole pair migrate to the surface of Cr-PTC-HIna for redox reaction. Photoexcited electrons reduce the oxygen into superoxide radicals that can be protonated by H^+ ion in water, forming hydroperoxyl radical (HO_2•) that eventually change into H_2O_2 that was dissociated into more reactive hydroxyl radical species OH• (iiib).

Hydrogen peroxide (H_2O_2) acts as an excited electron scavenger in the photocatalytic process, while CH_3OH acts as an electron-hole scavenger, and tert-butanol acts as a hydroxyl (•OH) radical scavenger. The results of the degradation measurements under various reaction conditions are shown in Figure 12.

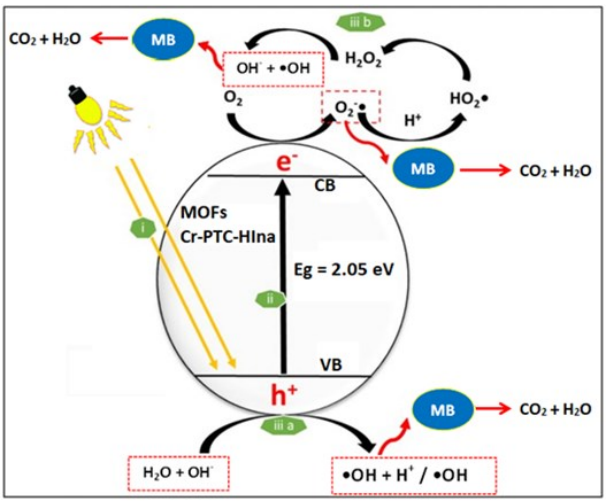

Figure 11. Photocatalytic methylene blue degradation mechanism by Cr-PTC-HIna under mercury lamp as visible light source.

Figure 12 illustrated that the addition of H_2O_2 increased the photocatalytic activity of Cr-PTC-HIna to degrade MB from 95.40 mg/gram to 129.06 mg/gram. Hydrogen peroxide in the system will capture excited electrons in the conduction band to reduce the rate of recombination between electrons and electron holes. H_2O_2 reacted with excited electrons to generate hydroxide ions (OH^-) and hydroxyl radicals (•OH). Furthermore, the electron holes in the valence band attract hydroxide ions (OH^-) and water (H_2O) to form hydroxyl radicals (•OH), wherein the hydroxyl radical will further react with methylene blue to form their oxidized products [27]. In addition, H_2O_2 itself was degraded directly by light to produce hydroxyl radicals (•OH). Thus, the addition of H_2O_2 prevents the recombination rate and increases the number of hydroxyl radical species (•OH) formation in the system so that more methylene blue is degraded (Equations 4-9).

On the other hand, Figure 12 explained the addition of tert-butanol and H_2O_2 originated lowering MB degradation from a solution that only added H_2O_2 from 129.06 mg/gram to 110.44 mg/gram. It confirmed that tert-butanol captures the hydroxyl radical species (•OH) in the system and brings on alighting the number of hydroxyl radical species (•OH) and involves a degression of methylene blue degradation.

$$MOFs + hv \rightarrow MOFs\ (e^-_{cb} + h^+_{vb}) \quad (4)$$
$$H_2O_2 + hv \rightarrow 2 \bullet OH \quad (5)$$
$$e^-_{cb} + H_2O_2 \rightarrow \bullet OH + OH^- \quad (6)$$
$$h^+_{vb} + OH^- \rightarrow \bullet OH \quad (7)$$
$$h^+_{vb} + H_2O \rightarrow \bullet OH + H^+ \quad (8)$$
$$MB + \bullet OH \rightarrow H_2O + CO_2 \quad (9)$$

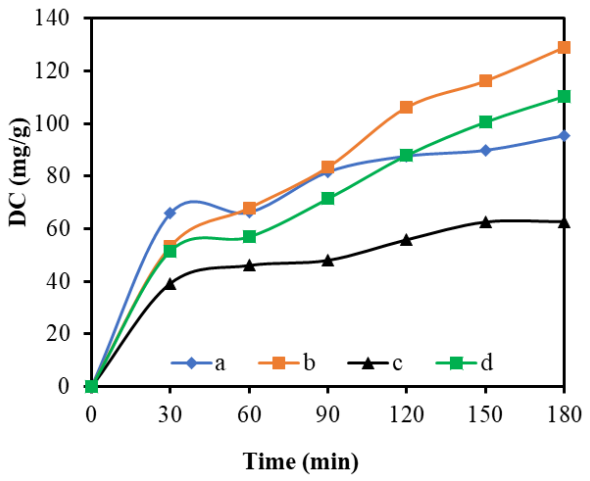

Figure 12. Degradation capacity of Cr-PTC-HIna in (a) MB; (b) MB+H_2O_2 0.2M; (c) MB+CH_3OH 0.2M; and (d) MB+H_2O_2 0.2M + tert-butanol 0.2M.

In contrast with H_2O_2, the addition of methanol caused a decrease in the degradation of methylene blue from 95.40 mg/gram to 62.71 mg/gram. Methanol in the system act as an electron-hole scavenger. The electron holes react with methanol to form hydroxyalkyl radicals (•CH_2OH) and are further oxidized to formaldehyde (CH_2O) [5]. Meanwhile, excited electrons in the conduction band react with oxygen to form superoxide radicals (•O_2^-) and further react with methylene blue to form degradation products (Equations 10-13). In this condition, the degradation of MB was just affected by radical superoxide. Fakhrul *et al*. argued that the degradation capability of hydroxyl radical species (•OH) is greater than superoxide radical (•O_2^-) [33]. Consequently, adding methanol affords less degradation efficiency than H_2O_2.

$$MOFs + hv \rightarrow MOFs\ (e^-_{cb} + h^+_{vb}) \quad (10)$$
$$h^+_{vb} + CH_3OH \rightarrow \bullet CH_2OH + CH_2O \quad (11)$$
$$e^-_{cb} + O_2 \rightarrow \bullet O_2 \quad (12)$$
$$MB + \bullet O_2^- \rightarrow H_2O + CO_2 \quad (13)$$

4. Conclusions

New responsive visible light MOF, Cr-PTC-HIna, was successfully synthesized by using solvothermal method. This material degrades methylene blue in optimum conditions at pH of 7, and mass of 25 mg in 50 mL MB solution under visible light irradiation with a degradation capacity of 95.40 mg/g for 180 min time reaction. The radical species that promote MB degradation by MOFs Cr-PTC-HIna is hydroxyl radicals.

Acknowledgments

The authors wish to thank UIN Syarif Hidayatullah Jakarta for financial support with the contract number B-301/LP2M-PUSLITPEN/TL.03/2022. In addition, thanks to Universitas Indonesia for facilitating to carrying out of this work.

References

[1] Wong, Y.C., Szeto, Y.S., Cheung, W.H., McKay, G. (2003). Equilibrium studies for acid dye adsorption onto chitosan. *Langmuir*, 19(19), 7888–7894. DOI: 10.1021/la030064y

[2] Illahi, A.N., Rouf, U.A., Maulidianingtyas, H., Hastuti, E., Prasetyo, A., Istighfarini, V.N. (2020). Sintesis dan karakterisasi material fotokatalis heterojunction $Bi_4Ti_3O_{12}$/$SrTiO_3$ dengan metode sonikasi. *Jurnal Kimia Riset*, 5(1), 36. DOI: 10.20473/jkr.v5i1.20196

[3] Yahya, N., Aziz, F., Jamaludin, N.A., Mutalib, M.A., Ismail, A.F., Salleh, W.N.W, Jaafar, J., Yusof, N., Ludin, N.A. (2018). A review of integrated photocatalyst adsor bents for wastewater treatment. *Journal of Environmental Chemical Engineering*, 6(6), 7411–7425. DOI: 10.1016/j.jece.2018.06.051

[4] Vyas, V.S., Lau, V.W.H., Lotsch, B.V. (2016). Soft Photocatalysis: Organic Polymers for Solar Fuel Production. *Chemistry of Materials*, 28(15), 5191–5204. DOI: 10.1021/acs.chemmater.6b01894

[5] Zulys, A., Adawiah, A., Gunlazuardi, J., Yudhi, M.D.L. (2021). Light-harvesting metal-organic frameworks (MOFs) La-PTC for photocatalytic dyes degradation. *Bulletin of Chemical Reaction Engineering & Catalysis*, 16(1), 170–178. DOI: 10.9767/bcrec.16.1.10309.170-178.

[6] Bumstead, A.M., Cordes, D.B., Dawson, D.M., Chakarova, K.K., Mihaylov, M.Y., Hobday, C.L., Düren, T., Hadjiivanov, K.I., Slawin, A.M.Z., Ashbrook, S.E., Prasad, R.R.R., Wright, P.A. (2018). Modulator-controlled synthesis of microporous STA-26, an interpenetrated 8,3-connected Zirconium MOF with the the-i topology, and its reversi ble lattice shift. *Chemistry - A European Journal*, 24(23), 6115–6126. DOI: 10.1002/chem.201705136

[7] Cai, G., Jiang, H.L. (2017). A Modulator-induced defect-formation strategy to hierarchically porous metal–organic frameworks with high stability. *Angewandte Chemie - International Edition*, 56(2), 563–567. DOI: 10.1002/anie.201610914

[8] Jiang, D., Zhu, Y., Chen, M., Huang, B., Zeng, G., Huang, D., Song, B., Qin, L., Wang, H., Wei, W. (2019). Modified crystal structure and improved photocatalytic activity of MIL-53 via inorganic acid modulator. *Applied Catalysis B: Environmental*, 255, 117746. DOI: 10.1016/j.apcatb.2019.117746

[9] Derivadas, I. (2020). Isonicotinic acid ≥ 99%, for synthesis Safety data sheet. In *IDESA Petroquimica*.

[10] Zhang, F.H., Wang, Y.Y., Lv, C., Li, Y.C., Zhao, X.Q. (2019). Luminescent complexes associated with isonicotinic acid. *Journal of Luminescence*, 207, 561–570. DOI: 10.1016/j.jlumin.2018.11.051

[11] Garibay, S.J., Lordanov, I., Islamoglu, T., DeCoste, J.B., Farha, O.K. (2018). Synthesis and functionalization of phase- pure NU-901 for enhanced CO_2 adsorption: The influence of zirconium salt and modulator on topology and phase purity. *CrystEngComm*, 2018, 20, 7066-7070. DOI: 10.1039/c8ce01454j

[12] Zhou, L., Fan, H., Zhou, B., Cui, Z., Qin, B., Zhang, X., Li, W., Zhang, J. (2019). Tetranuclear cobalt(II)-isonicotinic acid frameworks: selective CO_2 capture, magnetic properties, and derived "Co_3O_4" exhibiting high performance in lithium ion batteries. *Dalton Transactions*, 48(1), 296–303. DOI: 10.1039/c8dt04054k

[13] Yuan, S., Feng, L., Wang, K., Pang, J., Bosch, M., Lollar, C., Sun, Y., Qin, J., Yang, X.,Zhang, P., Wang, Q., Zou, L., Zhang, Y., Zhang, L., Fang, Y., Li, J., Zhou, H.C. (2018). Stable metal– organic frameworks: design, synthesis, and applications. *Advanced Materials*, 30(37), 1–35. DOI: 10.1002/adma.201704303

[14] Hasan, M. R. (2015). *Pengaruh Penambahan Modulator Asam Asetat Pada Sintesis Metal Organic Framework Tipe HKUST-1* (ITS). ITS. Retrieved from http://repository.its.ac.id/60094/

[15] Seetharaj, R., Vandana, P.V., Arya, P., Mathew, S. (2019). Dependence of solvents, pH, molar ratio and temperature in tuning metal organic framework architecture. *Arabian Journal of Chemistry*, 12(3), 295–315. DOI: 10.1016/j.arabjc.2016.01.003

[16] Roosta, M., Ghaedi, M., Daneshfar, A., Sahraei, R., Asghari, A. (2014). Optimization of the ultrasonic assisted removal of methylene blue by gold nanoparticles loaded on activated carbon using experimental design methodology. *Ultrason. Sonochem.,* 21, 242–252. DOI: 10.1016/j.ultsonch.2013.05.014

[17] Li, D., Zhong, G. (2014). Synthesis , crystal structure , and thermal decomposition of the Cobalt(II) complex with 2-picolinic acid. *The Scientific World Journal*, 2014, 1–7. DOI: 10.1155/2014/641608

[18] Jiang, X., Zhang, L., Liu, S., Zhang, Y., He, Z., Li, W., Zhang, F., Shi, Y., Lü, W., Li, Y., Wen, Q., Li, J., Feng, J., Ruan., S., Zeng Y.J., Zhu, X., Lu, Y., Zhang, H. (2018). Ultrathin metal–organic framework: an emerging broadband nonlinear optical material for ultrafast photonics. *Advanced Optical Materials*, 6(16), 1–11. DOI: 10.1002/adom.201800561

[19] Zulys, A., Asrianti, D., Gunlazuardi, J. (2020). Synthesis and characterization of metal organic frameworks based on nickel and perylene dyes as water splitting photocatalyst. *AIP Conference Proceedings*, 2243, 5–9. DOI: 10.1063/5.0005001

[20] Lin, C.K., Zhao, D., Gao, W.Y., Yang, Z., Ye, J., Xu, T., Ge, Q., Ma, S., Liu, D.J. (2012). Tunability of band gaps in metal-organic frameworks. *Inorganic Chemistry*, 51 16), 9039–9044. DOI: 10.1021/ic301189m

[21] Adawiah, A., Yudhi, M.D.L., Zulys, A. (2021). Photocatalytic Degradation of Methylene Blue and Methyl Orange by Y-PTC Metal-Organic Framework. *Jurnal Kimia Valensi,* 7(1), 129-141. DOI: 10.15408/jkv.v7i2.22267

[22] Hoffman, A.J., Mills, G., Yee, H., Hoffmann, M.R. (1992). Q-sized CdS: Synthesis, characterization, and efficiency of photoinitiation of polymerization of several vinylic monomers. *Journal of Physical Chemistry*, 96(13), 5546–5552. DOI: 10.1021/j100192a067

[23] Mohanraj, V.J., Chen, Y. (2006). Nanoparticles – A Review. *Tropical Journal of Pharmaceutical Research*, 5 (1), 561-573. DOI: 10.4314/tjpr.v5i1.14634.

[24] Zhang, P., Wang, Q., Fang, Y., Chen, W., Kirchon, A.A., Baci, M., Feng, M., Sharma, V.K., Zhou, H.C. (2019). 7-Metal-organic frameworks for capture and degra dation of organic pollutants. In *Metal-Organic Frameworks (MOFs) for Environmental Applications*. Elsevier Inc.

[25] Rojas, S., Horcajada, P. (2020). Metal-Organic Frameworks for the Removal of Emerging Organic Contaminants in Water. *Chemical Reviews*, 120 (16), 8378–8415. DOI: 10.1021/acs.chemrev.9b00797

[26] Mantasha, I., Saleh, H.A.M., Qasem, K.M.A., Shahid, M., Mehtab, M., Ahmad, M. (2020). Efficient and selective adsorption and separation of methylene blue (MB) from mixture of dyes in aqueous environment employing a Cu(II) based metal organic framework. *Inorganica Chimica Acta*, 511, 119787. DOI: 10.1016/j.ica.2020.119787

[27] Wang, F., Guo, H., Chai, Y., Li, Y., Liu, C. (2013). The controlled regulation of morphology and size of HKUST-1 by coordination modulation method. *Microporous and Mesoporous Materials*, 173, 181–188. DOI: 10.1016/j.micromeso.2013.02.023

[28] Rondang, T., Limbong, H.P., Pinem, C., Manurung, E. (2017). Pengaruh Ukuran Partikel, Waktu dan Suhu Pada Ekstraksi Fenol dari Lengkuas Merah. *Jurnal Teknik Kimia USU*, 5 (4), 53–56. DOI: 10.32734/jtk.v5i4.1555

[29] Kudo, A., Miseki, Y. (2009). Heterogeneous photocatalyst materials for water splitting. *Chemical Society Reviews*, 38(1), 253–278. DOI: 10.1039/b800489g

[30] Samuel, M.S., Bhattacharya, J., Parthiban, C., Viswanathan, G., Pradeep Singh, N.D. (2018). Ultrasound-assisted synthesis of metal organic framework for the photocatalytic reduction of 4-nitrophenol under direct sunlight. *Ultrasonics Sonochemistry*, 49, 215–221. DOI: 10.1016/j.ultsonch.2018.08.004

[31] Krishnan, J., Arvind Kishore, A., Suresh, A., Madhumeetha, B., Gnana Prakash, D. (2017). Effect of pH, inoculum dose and initial dye concentration on the removal of azo dye mixture under aerobic conditions. *International Biodeterioration and Biodegradation*, 119, 16–27. DOI: 10.1016/j.ibiod.2016.11.024

[32] Kumar, A. (2017). A Review on the factors affecting the photocatalytic degradation of hazardous materials. *Material Science & Engineering International Journal*, 1(3), 106–114. DOI: 10.15406/mseij.2017.01.00018

[33] Samsudin, M.F.R., Siang, L.T., Sufian, S., Bashiri, R., Mohamed, N.M., Ramli, R.M. (2018). Exploring the role of electron-hole scavengers on optimizing the photocatalytic performance of $BiVO_4$. *Materials Today: Proceedings*, 5 (10), 21703–21709. DOI: 10.1016/j.matpr.2018.07.022